

Theoretical investigation of structure and magnetic property of cubic MgFe_2O_4

B. Khongorzul^{1,2}, N. Tsogbadrakh^{1,*} and D. Sangaa²

¹*Department of Physics, School of Arts and Sciences,*

National University of Mongolia, Ulaanbaatar 14201, Mongolia

²*Institute of Physics and Technology, Mongolian Academy of Science, Ulaanbaatar 13330, Mongolia*

Spinel type ferrites are of interest for many applications to their magnetic ion occupation induced magnetic phase transition. We consider the stability of ground states and magnetic property of normal, half and full inversed spinel structures for cubic MgFe_2O_4 phase using the first - principles method within the framework of density functional theory with on site correction for Coulomb interaction (GGA + U + J_0). We have predicted the lattice parameters, magnetic moments of magnetic ions and compared with the results of x - ray diffraction and neutron scattering measurements.

PACS numbers: 75.10.Dg, 75.50.Gg

I. INTRODUCTION

Three basic classes of ferrites are made into magnetic ceramic products. Based upon their crystal structure, they are the spinel type ferrites, hexagonal type ferrites, and garnets. Iron containing spinels have the formula $\text{M}(\text{Fe}_2\text{O}_4)$, where M is usually a divalent cation such as manganese (Mn^{2+}), nickel (Ni^{2+}), cobalt (Co^{2+}), zinc (Zn^{2+}), copper (Cu^{2+}) or magnesium (Mg^{2+}). M can also represent the monovalent lithium cation (Li^+) or even vacancies, as long as these absences of positive charge are compensated for by additional trivalent iron cations (Fe^{3+}). The oxygen anions (O^{2-}) adopt a close - packed cubic crystal structure, and the metal cations occupy the interstices in an unusual two - lattice arrangement.

Magnesium ferrite (MgFe_2O_4) is an important magnetic oxide with spinel structure. Magnesium ferrite and allied compounds have found wide spread applications in microwave device because of their low magnetic and dielectric losses and high resistivity. MgFe_2O_4 enjoys special attention for many application, such as circulators, insulator, phase shifters, high density recording media, heterogeneous catalysis, sensors and good photoelectric effect. Synthesis of MgFe_2O_4 nanoparticle has been attempted by several investigators. Though numbers of research papers are available in the literature on MgFe_2O_4 , synthesis of nanoferrites by chemical method is still considered to be in the infancy state in terms of reproducibility and further improvement [1]. Thermal coagulation therapy can be realized by application of an AC magnetic field from external coils to cancer tumors using magnetic ferrite materials. Up to now, the magnetite (Fe_3O_4) have been mainly investigated as the candidate material for this type of therapy [2-5].

In fact, their magnetic properties highly depend

upon the cation distribution in the basic cubic spinel structure (Space group $\text{Fd}\bar{3}\text{m}$, no 227). In the conventional unit cell, there are 54 atoms and the 8 Mg cations are coordinated by 4 oxygens (tetrahedral sites, Tet), and the 16 Fe cations are coordinated by 6 oxygens (octahedral sites, Oct). The antiparallel alignment and incomplete cancellation of magnetic spins between the two sublattices leads to a permanent magnetic moment. Because spinels are cubic in structure, with no preferred direction of magnetization, they are “soft” magnetically; i.e., it is relatively easy to change the direction of magnetization through the application of an external magnetic field.

The cubic spinel structures might have a structure that is in between the normal and inversed spinel structures. Hence, in general, the formula of spinel ferrite structures can be written as $(\text{M}_{1-\delta}^{2+}\text{Fe}_{\delta}^{3+})^{\text{Tet}}[\text{M}_{\delta}^{2+}\text{Fe}_{2-\delta}^{3+}]^{\text{Oct}}\text{O}_4$. The variable δ is called the degree of inversion and represents the proportion of Fe^{3+} occupying the tetrahedral sites. An inversion parameter defined as the amount of trivalent cation at the tetrahedral sites (8a) is used to identify whether a spinel oxide forms in one of either largely normal or largely inverse structures. For $\delta = 0$, we can obtain $(\text{M}^{2+})^{\text{Tet}}[\text{Fe}_2^{3+}]^{\text{Oct}}\text{O}_4$, which is the normal spinel structure. For $\delta = 0.5$, we can obtain $(\text{M}_{0.5}^{2+}\text{Fe}_{0.5}^{3+})^{\text{Tet}}[\text{M}_{0.5}^{2+}\text{Fe}_{1.5}^{3+}]^{\text{Oct}}\text{O}_4$, which is the half inversed spinel structure. For $\delta = 1$, we can obtain $(\text{Fe}^{3+})^{\text{Tet}}[\text{M}^{2+}\text{Fe}^{3+}]^{\text{Oct}}\text{O}_4$, which is the full inversed spinel structure. They are usually accepted among the community that a normal spinel structure is formed for $0 < \delta < 2/3$ while an inverse spinel structure is stabilized with $2/3 < \delta < 1$ [3, 6].

While the tetrahedral site of the spinel structure forms a diamond lattice. The octahedral site forms pyrochlore lattice. In the normal spinel, this pyrochlore lattice hosts a three dimensional network of corner - sharing tetrahedral, which for antiferromagnetic (AFM) interactions gives rise to intrinsic geometric frustration leading to novel emergent properties such as spin ice, cluster glass, etc [7]. For the inversed spinel, the magnetic Fe ions are distributing

*Electronic address: Tsogbadrakh@num.edu.mn

on both the diamond and pyrochlore sublattices and the frustration is therefore breaking.

In this article, we consider the structure and magnetic property of normal, half and full spinel structures for cubic MgFe_2O_4 phase using the GGA + U + J_0 method (static mean field theory (MFT)) within the density functional theory (DFT) [8–10].

II. CALCULATION DETAILS

We considered the three cases: normal, half and full inversed spinels of the cubic MgFe_2O_4 phase. We have shown the primitive unit cell of normal MgFe_2O_4 spinel in the Figure 1 (See Appendix A). We have created the half and full inversed spinel structures by exchanging the magnetic Fe^{3+} ion with minority spin as Mg^{2+} ions.

Our calculations are based on the pseudopotential plane wave self-consistent field (PWscf) method using the generalized gradient approximation (GGA) by Perdew and Wang (PW91) [11] within the framework of DFT [8–10], as implemented in the QUANTUM ESPRESSO package [12]. The interaction between the ions and valence electrons is expressed as the ultrasoft pseudopotential [13]. The following electronic states are treated as valence states: $\text{O}(2s^2, 2p^4)$, $\text{Mg}(2p^6, 3s^1, 3p^{0.75})$ and $\text{Fe}(3s^2, 3p^6, 3d^{6.5}, 4s^1)$. The wave functions are expressed as plane waves up to a kinetic energy cutoff of 40 Ry and the kinetic energy cutoff for charge density and potential is chosen by 320 Ry. Three dimensional Fast Fourier Transform (FFT) meshes for charge density, scf potential and wavefunction FFT and smooth part of charge density are chosen to be $(70 \times 70 \times 70)$ grids. There might be need to use finer k -points meshes for a better evaluation of on-site occupations due the strong correlated system. The summation of charge densities is carried out using the special k -points restricted by the $(5 \times 5 \times 5)$ grids of Monkhorst - Pack scheme due to the computer power ability [14]. The tetrahedral method is used when the electronic densities of state (DOS) are evaluated [15]. To obtain optimized atomic structures, ionic positions and lattice parameters are fully relaxed until the residual forces are less than $0.05 \text{ eV}/\text{\AA}$ for each atom. The occupation numbers of electrons are expressed Gaussian distribution function with an electronic temperature of $kT = 0.02 \text{ Ry}$. The mixing mode of charge density is chosen to be local density independent Tomas - Fermi (TF) screening for highly inhomogeneous systems. Its mixing factor for self-consistency is to be 0.2 and the number of iterations used in mixing scheme is 5. The generalized eigenvalue problem is solved by the iterative diagonalization using the conjugate gradient (CG) minimization technique, and the starting wave function is chosen from superposition of atomic orbitals plus

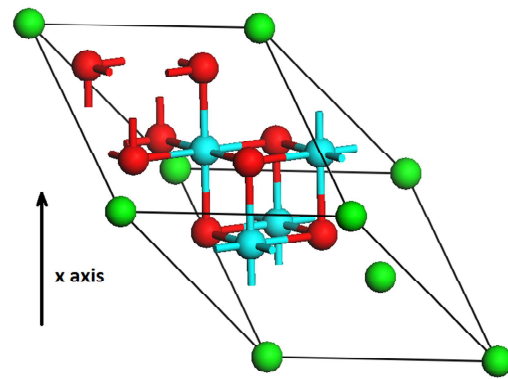


FIG. 1: (Color online) The primitive unit cell of normal MgFe_2O_4 spinel. The Mg, Fe and O atoms are green, blue and red balls respectively.

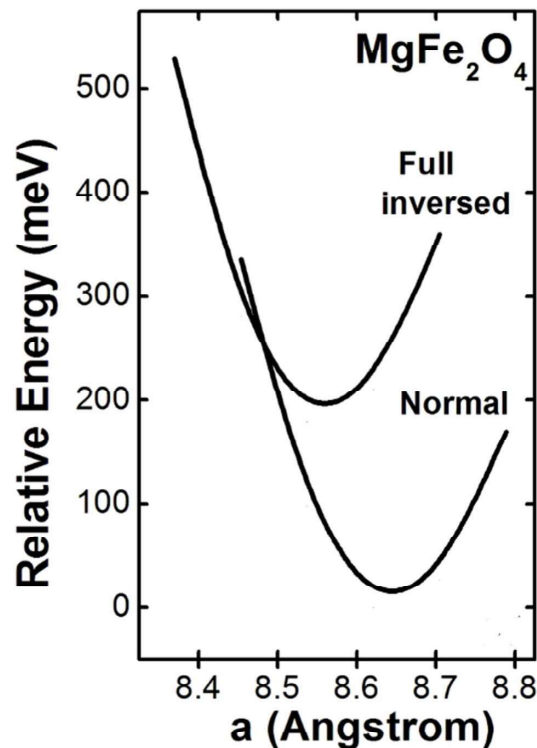


FIG. 2: The relative energy of ground state of MgFe_2O_4 as a function of lattice parameter.

a superimposed "randomization" of atomic orbitals in all our calculation [12, 16]. By the static MFT, in order to express the strong correlated effect of electrons in the $\text{Fe}(3d)$ state, we used the extended Hubbard based Hamiltonian including the effective magnetic exchange interaction parameter J_0 and the on-site Coulomb interaction is chosen to be $U = 7.5 \text{ eV}$ using the simplified rotational invariant formulation based on the linear response method [17]. The Hubbard parameter, which is used to the perturbation to compute J_0 with the linear response method, is chosen to be 1 eV [18]. Atomic wavefunctions used

for GGA + U + J_0 projector are not orthogonalized.

III. RESULTS AND DISCUSSION

We have first performed the calculations of atomic optimizations of normal, half and full inversed spinel structures for cubic MgFe_2O_4 phase. We predicted the lattice parameters to be 8.62, 8.54 and 8.54 Å in the normal, half and full inversed spinel structures respectively (See Table I). Overall, our predicted structure properties are close the other experimental results by the X-ray diffraction (XRD) and neutron diffraction measurements [19, 20]. The lattice parameters are same each other. It is related to the internal diffusion process of cation atoms. The degree of inversion for cubic MgFe_2O_4 phase is experimentally determined to be 0.82 by the neutron scattering measurement, and it is shown us to be full inversed spinel structure [20]. We note that the sample preparation of full normal and inversed structures for MgFe_2O_4 phase is too difficult to obtain these spinel ferrites.

The ground state of normal spinel structure for cubic MgFe_2O_4 phase is favored than that of the inversed spinel structures and the ground states of half and full inversed spinel structures are energetically increased by 299.97 and 179.12 meV/cell respectively. We have shown the relative energy as function of lattice parameter in Figure 2. In the normal spinel structure, the Mg^{2+} atoms are occupying on the tetrahedral sites, while Fe^{3+} atoms are occupying on the octahedral sites. When the Mg^{2+} and Fe^{3+} atoms consist of equal numbers of divalent and trivalent elements, distributed over crystallographically equivalent B1 and B2 octahedral sites, then the spinel structure is referred to as a full inverse spinel kind. We assume that the high temperature limit of cubic MgFe_2O_4 phase is known to have the full inverse spinel structure, where the atoms on the tetrahedral sites are Fe^{3+} ions, and octahedral sites are equally populated by Mg^{2+} and Fe^{3+} ions due to the migration of Mg^{2+} and Fe^{3+} ions from the tetrahedral site to octahedral site [21].

After the structure stably, we have performed the first - principles spin polarized calculations of ferromagnetic (FM), AFM and ferrimagnetic (FIM) states on the normal, half and full inversed spinel structures for cubic MgFe_2O_4 phase. The magnetic property of cubic MgFe_2O_4 phase creates from the magnetic Fe^{3+} ions and the magnetic ion of normal $(\text{Mg})^{\text{Tet}}[\text{Fe}_2]^{\text{Oct}}\text{O}_4$ spinel structure is sited on the pyrochlore sublattice. The spin orientations of the magnetic ions are corner sharing sited on the pyrochlore sublattice and the number of magnetic ions with majority and minority spin states is equal each other. Therefore the AFM states are stabilized and degenerated due

to the frustrated cubic MgFe_2O_4 phase [7]. For the half inversed $(\text{Mg}_{0.5}\text{Fe}_{0.5})^{\text{Tet}}[\text{Mg}_{0.5}\text{Fe}_{1.5}]^{\text{Oct}}\text{O}_4$ spinel structure consists of face - centered cubic close - packed oxygen sublattice and in which a fraction of tetrahedral and octahedral sites are filled by Mg^{2+} ions. For the full inversed $(\text{Fe})^{\text{Tet}}[\text{MgFe}]^{\text{Oct}}\text{O}_4$ spinel structure, the pyrochlore sublattice is destroyed and the magnetic Fe^{3+} ions are sited on both the tetrahedron and octahedron positions.

In our calculations, for the normal spinel structure, the magnetic moments of majority and minority states for Fe^{3+} ions are found to be 4.03 and -4.35 μ_B /atom respectively. In half inversed spinel structure, the magnetic moments of majority and minority states for Fe^{3+} ions are found to be 4.00 and -4.36 μ_B /atom respectively. For the full inversed spinel structure, the magnetic moments of majority and minority states for Fe^{3+} ions are found to be 3.99 and -4.35 μ_B /atom respectively. The magnetic moments of Fe^{3+} ions in the full inversed structure agree with the results of neutron scattering measurement of MgFe_2O_4 [22]. We have also shown the induced magnetic moments of non magnetic ions in the Table I. Their magnetic state is found to be AFM and the magnetic energy gains ΔE ($\Delta E = E_{\text{tot}}[\text{FM}] - E_{\text{tot}}[\text{AFM}]$) between the FM and AFM states are found to be 15.56, 15.91 and 16.28 eV/cell in the normal, half and full inversed spinel structures respectively. For the full inversed spinel structure, we found that the degeneration of AFM states destroyed and the energy differences of their spin orientations are found up to 0.512 meV/cell.

IV. CONCLUSION

In conclusion, we have presented the main results of structure and magnetic property of normal, half and full inversed spinel structures for cubic MgFe_2O_4 phase using the first - principles method with the static MFT within the framework of DFT. We have predicted that the ground state of normal spinel structure for cubic MgFe_2O_4 phase is favored than that of the half and full inversed spinel structures. For the magnetic property, we have shown that the magnetic moments of Fe^{3+} ions in the full inversed structure agree with the results of neutron scattering measurement of MgFe_2O_4 .

Acknowledgments

This work was supported by the Mongolian Foundation of Science and Technology (Grant N12-02-92200). We thanks for performing the calculations on the server computers generated by the (SST 031/2015) project at the School of Engineering and

Applied Science in the National University of Mongolia.

V. APPENDIX

A. Definition of coordinate frame

The cubic MgFe_2O_4 spinel structure consists of the two sublattices and the simplex lattice of pyrochlore lattice creates the diamond lattice. Therefore our structure crystallizes in the face - centered cubic structure and we describe the basis sets of primitive unit cell in the Cartesian coordinate frame as following

$$\vec{a}_1 = \frac{1}{2}a \begin{pmatrix} 0 \\ 1 \\ 1 \end{pmatrix}; \quad (1)$$

$$\vec{a}_2 = \frac{1}{2}a \begin{pmatrix} 1 \\ 0 \\ 1 \end{pmatrix}; \quad (2)$$

$$\vec{a}_3 = \frac{1}{2}a \begin{pmatrix} 1 \\ 1 \\ 0 \end{pmatrix} \quad (3)$$

and the positions of the Mg and Fe atoms for normal MgFe_2O_4 spinel on the tetrahedral and octohedral sites respectively are defined as:

$$\vec{r}_{Mg_1} = \frac{1}{8}a \begin{pmatrix} 0 \\ 0 \\ 0 \end{pmatrix}; \quad (4)$$

$$\vec{r}_{Mg_2} = \frac{1}{8}a \begin{pmatrix} 2 \\ 2 \\ 2 \end{pmatrix} = \frac{1}{8}(\vec{a}_1 + \vec{a}_2 + \vec{a}_3) \quad (5)$$

$$\vec{r}_{Fe_1} = \frac{1}{8}a \begin{pmatrix} 1 \\ 5 \\ 5 \end{pmatrix} = \frac{1}{8}(9\vec{a}_1 + \vec{a}_2 + \vec{a}_3); \quad (6)$$

$$\vec{r}_{Fe_2} = \frac{1}{8}a \begin{pmatrix} 5 \\ 1 \\ 5 \end{pmatrix} = \frac{1}{8}(\vec{a}_1 + 9\vec{a}_2 + \vec{a}_3) \quad (7)$$

$$\vec{r}_{Fe_3} = \frac{1}{8}a \begin{pmatrix} 5 \\ 5 \\ 1 \end{pmatrix} = \frac{1}{8}(\vec{a}_1 + \vec{a}_2 + 9\vec{a}_3); \quad (8)$$

$$\vec{r}_{Fe_4} = \frac{1}{8}a \begin{pmatrix} 5 \\ 5 \\ 5 \end{pmatrix} = \frac{5}{8}(\vec{a}_1 + \vec{a}_2 + \vec{a}_3) \quad (9)$$

where a is the lattice parameter of cubic structure in the conventional unit cell with the pyrochlore lattice.

-
- [1] S. M. Hoque, M. A. Hakim, A. Mamun, S. Akhter, M. T. Hasan, D. P. Paul and K. Chattopadhyay, *Mater. Sci. and Appl.* **2**, 1564 (2011).
 - [2] M. Ma, Y. Wu, J. Zhou, Y. Sun, Y. Zhang and N. Gu, *J. Magn. Magn. Mater.* **268**, 33 (2004).
 - [3] T. Maehara, K. Konishi, T. Kamimori, H. Aono, H. Hirazawa, T. Naohara, S. Nomura, H. Kikkawa, Y. Watanabe and K. Kawachi, *J. Mater. Sci.* **40**, 135 (2005).
 - [4] H. Hirazawa, H. Aono, T. Naohara, T. Maehara, M. Sato and Y. Watanabe, *J. Magn. Magn. Mater.* **323**, 675 (2011).
 - [5] H. Hirazawa, Y. Ito, D. Sangaa, N. Tsogbadrakh, H. Aono and T. Naohara, *AIP, Conference Proceedings* **1763** 020009 (2016).
 - [6] G. Ferk, M. Drofenik, D. Lisjak, A. Hamler, Z. Jaglicic and D. Makovec, *J. Magn. Magn. Mater.* **350**, 124 (2014).
 - [7] Introduction to Frustrated Magnetism, *Edited by C. Lacroix, P. Mendels and F. Mila*, Springer, (2011).
 - [8] P. Hohenberg and W. Kohn, *Phys. Rev.* **136**, B864 (1964).
 - [9] W. Kohn and L. J. Sham, *Phys. Rev.* **140**, A1133 (1965).
 - [10] R. O. Jones and O. Gunnarsson, *Rev. Mod. Phys.* **61** 689 (1989).
 - [11] J. P. Perdew, J. A. Chevary, S. H. Vosko, Koblar A. Jackson, M. R. Pederson, D. J. Singh and C. Fiolhais, *Phys. Rev. B* **46**, 6671 (1992).
 - [12] P. Gianmazzi, S. Baroni, N. Bonini, M. Calandra, R. Car, C. Cavazzoni, D. Ceresoli, G. L. Chiarotti, M. Cococcioni, I. Dabo, A. D. Corso, S. de Gironcoli, S. Fabris, G. Fratesi, R. Gebauer, U. Gerstmann, C. Gougoussis, A. Kokalj, M. Lazzeri, L. Martin-Samos, N. Marzari, F. Mauri, R. Mazzarello, S. Paolini, A. Pasquarello, L. Paulatto, C. Sbraccia, S. Scandolo, G. Sclauzero, A. P. Seitsonen, A. Smogunov, P. Umari and R. M. Wentzcovich, *J. Phys.: Condens. Matter* **21**, 395502 (2009).
 - [13] D. Vanderbilt, *Phys. Rev. B* **41**, 7892 (1990).
 - [14] H. J. Monkhorst and J. D. Pack, *Phys. Rev. B* **13**, 5188 (1976).
 - [15] P. E. Blochl, O. Jepsen and O. K. Andersen, *Phys. Rev. B* **49**, 16223 (1994).

TABLE I: For the cubic $MgFe_2O_4$ phase, degree of inversion, optimized lattice parameters, stability energy gains δE (units of meV/cell) for the AFM states between the half inversed (HI) / full inversed (FI) and the normal (N) spinels ($\delta E = E_{tot}[AFM](MI/FI) - E_{tot}[AFM](N)$), magnetic energy gains ΔE (units of eV/cell) for each spinel structures ($\Delta E = E_{tot}[FM] - E_{tot}[AFM]$), magnetic moments (units of μ_B /atom) of each atomic site and total magnetizations (units of μ_B /cell) normal, half and full inversed spinel structures for cubic $(Mg_{1-\delta}Fe_{\delta})_A[Mg_{\delta}Fe_{2-\delta}]_BO_4$ ($\delta = 0, 0.5$ and 1) phase using the GGA + U + J_0 method (static MFT). The experimental lattice parameters and magnetic moments of Fe^{3+} ions are in the last column [19, 20, 22].

	$(Mg)^{Tet}[Fe_2]^{Oct}O_4$	$(Mg_{0.5}Fe_{0.5})^{Tet}[Mg_{0.5}Fe_{1.5}]^{Oct}O_4$	$(Fe)^{Tet}[MgFe]^{Oct}O_4$	Exp.
δ	0	0.5	1.0	0.82 [20]
a (Å)	8.62	8.54	8.54	8.40 [19], 8.38 [20]
δE	0	299.97	179.12	
ΔE	15.56	15.91	16.28	
M(Mg)	-0.001	0.007	-0.009	
M(Fe_1)	4.034	4.004	3.988	3.8 [22]
M(Fe_2)	-4.348	-4.362	-4.353	-4.4 [22]
M(O_1)	0.210	0.057	0.176	
M(O_2)	-0.047	-0.076	0.019	
M(O_3)	0.210	0.057	0.176	
M(O_4)	-0.047	-0.076	0.019	
M(Total)	0.00	0.00	0.00	

- [16] M. C. Payne, M. P. Teter, D. C. Allan, T. A. Arias and J. D. Joannopoulos, Rev. Mod. Phys. **64**, 1045 (1992).
[17] M. Cococcioni and S. de Gironcoli, Phys. Rev. B. **71**, 035105 (2005).
[18] B. Hummetoglu, R. M. Wentzcovich and M. Cococcioni, Phys. Rev. B **84**, 115108 (2011).
[19] J. P. Singh, S. O. Won, W. C. Lim, I. J. Lee and K. H. Chae, J. Mol. Struc. **108**, 444 (2016).
[20] E. Uyanga, D. Sangaa, H. Hirazawa, N. Tsog-

- badrakh, N. Jargalan, I.A.Bobrikov and A.M. Balagurov, Mat. Res. Bull. (Submitted in 2017).
[21] C. L. Muhich, V. J. Aston, R. M. Trottier, A. W. Weimer and C. B. Musgrave, Chem. Mater. **28**, 214 (2016).
[22] D. Sangaa, B. Khongorzul, E. Uyanga, N. Jargalan, N. Tsogbadrakh and H. Hirazawa, Sol. Stat. Phen. (Submitted in 2017).